

On the Excitation of Leaky Modes in Cylindrical Loops

J. Terradas · J. Andries · M. Goossens

Received: 12 January 2007 / Accepted: 3 October 2007 / Published online: 3 November 2007
© Springer Science+Business Media B.V. 2007

Abstract The role of leaky waves in the coronal loop oscillations observed by TRACE is not yet clearly understood. In this work, the excitation of fast waves in solar coronal loops modelled as dense plasma cylindrical tubes in a uniform straight magnetic field is investigated. We study the trapped and especially leaky modes (whose energy escapes from the tube) that result from an initial disturbance by solving the time-dependent problem numerically. We find that the stationary state of the tube motion is given by the trapped normal modes. By contrast, the transient behaviour between the initial and the stationary phase is dominated by wave leakage. The so-called trig leaky modes are clearly identified since the transient behaviour shows periods and damping times that are in agreement with the values calculated from the normal-mode analysis. Consequently, these radiating modes have physical significance. However, we have not found any evidence for the excitation of other types of modes, such as the principal leaky kink mode.

Keywords MHD · Sun: corona · Sun: magnetic fields · Waves

1. Introduction

Coronal loop oscillations have become a hot topic since their direct observational detection with the *Transition Region and Coronal Explorer* (TRACE) (see Aschwanden *et al.*, 1999, 2002; Schrijver, Aschwanden, and Title, 2002). Long before their observation, the theory of loop oscillations was developed (Spruit, 1982; Edwin and Roberts, 1983; Cally, 1986) and the different kinds of oscillations, trapped and leaky modes, were studied. In particular, Cally (1986) and more recently Cally (2003) have pointed out that there are solutions of the dispersion relation, the so-called principal fast leaky modes (PFLK), that

J. Andries is postdoctoral Fellow of the National Fund for Scientific Research–Flanders (Belgium) (F.W.O.-Vlaanderen).

J. Terradas (✉) · J. Andries · M. Goossens
Centre for Plasma Astrophysics, Katholieke Universiteit Leuven, Celestijnenlaan 200B, 3001 Leuven, Belgium
e-mail: jaume@wis.kuleuven.be

can decay rapidly (although not fast enough) to be of interest because these modes could be a possible explanation of the observed damping of the transversal loop oscillations. However, Ruderman and Roberts (2006a) have solved the initial-value problem for the tube oscillations and claim that the principal leaky mode and many other leaky modes are unphysical. The role and the physical relevance of the leaky modes is still under debate (Cally, 2006; Ruderman and Roberts, 2006b). The problem arises from the fact that the dispersion function is multivalued in the complex frequency plane. The discussion is whether only the solutions on a certain Riemann sheet (the physical Riemann sheet, *i.e.*, determined by the conditions that solutions vanish at infinity) are physically relevant, or whether any physical relevance can be attributed to solutions on neighbouring Riemann sheets.

However, Andries and Goossens (2007) have pointed out that also in an unbounded physical domain the magnetohydrodynamic (MHD) operator remains self-adjoint and therefore eigenmodes should necessarily have real frequencies. The discussion about the Riemann sheets can be avoided by recasting the contribution of the branch cut in the initial-value problem (IVP) in the form of a continuous part in a complete spectral representation. It was shown in an MHD slab model that the spectral measure associated with this leaky continuum has bumps that are related to the solutions of the dispersion relation on the next Riemann sheet. These damped leaky solutions (Wilson, 1981; Spruit, 1982; Cally, 1986, 2003; Stenuit, Keppens, and Goossens, 1998; Stenuit *et al.*, 1999) are thus to be interpreted in the sense of quasi-modes as in the theories of resonant absorption or Landau damping.

An alternative and direct way to study the issue of the leaky modes is, given an initial perturbation, to solve the full time-dependent problem numerically and to study the behaviour of the system for all times. In particular, we can investigate in detail the possible excitation of the radiating modes from the evolution of the system. This approach has already been used by Terradas, Oliver, and Ballester (2005a) for a simple slab model. In this work, it was clearly shown for the first time that the transient behaviour before the loop settles in the trapped mode is characterised by the excitation of leaky modes. More recently, Pascoe, Nakariakov, and Arber (2007) have studied leaky and trapped sausage modes also for the slab model.

The main goal of the present paper is to extend the work of Terradas, Oliver, and Ballester (2005a) to a cylindrical loop model. This equilibrium introduces a richer spectrum of modes, especially the PFLK, which does not exist in the slab geometry and is the main point of controversy. The paper is organised as follows. In Section 2 the cylindrical loop model is described and the MHD equations are introduced. In Section 3 the main properties of the trapped and especially the leaky modes are briefly described. The initial perturbation and the method to solve the time-dependent problem is explained in Section 4. The results for the sausage and kink modes are shown in Section 5 for different initial excitations. Finally, the main conclusions are drawn in Section 6.

2. Basic Equations

The equilibrium configuration used to model a coronal loop of radius R and length L consists of a homogeneous straight tube described in cylindrical coordinates. The density profile has a sharp transition between the tube (ρ_i) and the loop environment (ρ_e). The loop and the coronal environment are permeated by a vertical and uniform magnetic field ($\mathbf{B} = B_0 \mathbf{e}_z$). The Alfvén speed, $v_A = B_0 / \sqrt{\mu_0 \rho}$, takes the values v_{Ai} inside the loop and v_{Ae} in the surrounding coronal medium ($v_{Ae} > v_{Ai}$ since $\rho_e < \rho_i$). We study linear perturbations of this

equilibrium in the zero- β limit and we use the ideal MHD equations

$$\frac{\partial v_r}{\partial t} = \frac{B_0}{\mu_0 \rho} \left(-ik_z b_r - \frac{\partial b_z}{\partial r} \right), \tag{1}$$

$$\frac{\partial v_\theta}{\partial t} = \frac{B_0}{\mu_0 \rho} \left(-ik_z b_\theta - \frac{im}{r} b_z \right), \tag{2}$$

$$\frac{\partial b_r}{\partial t} = -B_0 ik_z v_r, \tag{3}$$

$$\frac{\partial b_\theta}{\partial t} = -B_0 ik_z v_\theta, \tag{4}$$

$$\frac{\partial b_z}{\partial t} = -B_0 \frac{1}{r} \left(v_r + r \frac{\partial v_r}{\partial r} + im v_\theta \right), \tag{5}$$

where $\mathbf{v} = (v_r, v_\theta, 0)$ is the velocity and $\mathbf{b} = (b_r, b_\theta, b_z)$ is the perturbed magnetic field. In the equations we have Fourier analysed in the z direction (*i.e.*, we have assumed that the perturbations are of the form $e^{-ik_z z}$). We concentrate on the fundamental mode, with $k_z = \pi/L$. We have also assumed an azimuthal dependence of the form $e^{im\theta}$, with θ being the polar angle. The z and θ dependence considerably simplifies the problem because all the variables only depend on the radial coordinate r . Finally, note that since $\beta = 0$ slow modes are absent ($v_z = 0$).

3. Tube Eigenmodes

The main properties of the loop eigenmodes using a straight cylindrical-tube model have been studied by Spruit (1982), Edwin and Roberts (1983), Cally (1986, 2003), Stenuit, Kep-pens, and Goossens (1998) and Stenuit *et al.* (1999). Some of these works have focused on the trapped solutions, whereas others have also studied the leaky or radiating solutions. The trapped solutions correspond to standing oscillations of the tube. These modes have a real frequency and the eigenfunction tends to zero in the limit of $r \rightarrow \infty$. However, the leaky modes have a complex frequency and, strictly speaking, they are not normal modes of the system because their amplitude outside the tube increases with the distance from the loop.

The frequency of the trapped and leaky modes is calculated from the dispersion relation [see, for example, Equation (2) in Cally, 2003]. In the long-wavelength limit the kink mode and the fluting modes are trapped. In contrast, the sausage mode is leaky in this limit and is only trapped for longitudinal wavenumbers larger than a cutoff value (see Edwin and Roberts, 1983, and Roberts, Edwin and Benz, 1984). The eigenfrequency of the trapped solutions is always between the external ($\omega_{Ac} = v_{Ac} k_z$) and the internal cutoff frequencies ($\omega_{Ai} = v_{Ai} k_z$). However, in the thin-tube regime, the leaky modes can be basically classified into two types: modes that have the real part of the frequency above ω_{Ac} and solutions that are below this cutoff frequency (see, for example, Figure 1 in Cally, 2003).

The solutions that are above the external cutoff represent radially propagating fast waves. These modes, referred to as ‘‘trig’’ modes according to Cally (1986, 2003), have the follow-ing period:

$$P \approx \frac{4R}{\left(m + 2n + \frac{3}{2}\right)v_{Ai}}, \tag{6}$$

where n is any integer consistent with $P > 0$. Their damping time is

$$\tau_d \approx R v_{Ac} / v_{Ai}^2. \tag{7}$$

The previous expressions are only valid for $v_{Ai} \ll v_{Ac}$ and for thin and long loops. Note that for these leaky modes the period and damping time are independent of the loop length. Additionally, there is another family of trig leaky modes, the ‘‘Type II trig modes’’ (see Cally, 2006). These modes are solutions of the dispersion relation but with negative real frequency and a much faster attenuation than the ordinary trig modes. Another interesting leaky mode is the ‘‘orphan mode’’ which has a damping time similar to that of the Type II trig modes but a positive frequency (which is smaller than the frequency of the fundamental trig mode).

In contrast, the leaky solution that is below the external cutoff frequency is the principal kink leaky mode (Cally, 2003). This radiating wave basically oscillates with the period of the kink mode,

$$P \approx \frac{\sqrt{2}\pi}{k_z v_{Ai}}, \tag{8}$$

and the damping time is

$$\tau_d \approx \frac{4\sqrt{2}}{\pi k_z^3 R^2 v_{Ai}}. \tag{9}$$

The mode is a bifurcation branch of the trapped solution and $k_z R = 0$. Again, the previous expressions are only valid for thin long tubes and for $v_{Ai} \ll v_{Ac}$. For short and fat loops the frequency of this mode is quite different from the kink frequency. As noted by Cally (2003), this mode propagates almost parallel to the tube since the radial propagation speed is very small in comparison with the longitudinal wave speed (in the thin-tube regime).

4. Initial Perturbation and Method

Because we wish to investigate some time-varying aspects of our linear system, we suppose that the system is excited in a particular manner at a particular position. Specifically, we assume a disturbance located in the coronal medium and with the following form:

$$v_r(r, t = 0) = v_{r0} e^{-\left(\frac{r-r_0}{w}\right)^2} \cos k_r(r - r_0), \tag{10}$$

where v_{r0} is the amplitude of the perturbation, r_0 is the position of the centre of the disturbance, w is the width of the Gaussian at half height, and k_r is the characteristic wavenumber of the sinusoidal function. All other MHD variables are initially set to zero.

The initial perturbation represents a localised disturbance with a dominant wavenumber k_r . This can be seen from its Fourier transform

$$\begin{aligned} F(k) &= \int_{-\infty}^{\infty} v_r(r, t = 0) e^{-ikr} dr \\ &= v_{r0} \frac{\sqrt{\pi}}{2} \text{Erf}(1) w e^{-ikr_0} \left[e^{-\frac{w^2}{4}(k+k_r)^2} + e^{-\frac{w^2}{4}(k-k_r)^2} \right], \end{aligned} \tag{11}$$

where Erf is the error function. We see that $|F(k)|$ is large for values around $\pm k_r$, and the wider the perturbation is in space the more localised it is in k since the width of the Gaussian

in the Fourier transform is $2/w$. The initial perturbation in terms of the Fourier transform is simply

$$v_r(r, t = 0) = \frac{1}{2\pi} \int_{-\infty}^{\infty} F(k) e^{ikr} dk. \quad (12)$$

To numerically solve Equations (1)–(5) together with the initial perturbation given by Equation (10), we have used the time-dependent version of the PDE2D code (Sewell, 2005). The code makes use of a second-order Crank–Nicolson method with adaptive time step control. Because we are considering a finite numerical domain, reflections at the domain boundaries may affect the dynamics of the loop. To avoid this problem we have located the edges of the numerical domain far from the loop. Given that the size of the domain is much larger than the loop thickness, we have used a nonuniform grid with 1000 grid points in the full domain and typically 100 points inside the tube. In addition, we have ensured that the artificial diffusion introduced by the numerical scheme is small enough. Hence, the physical damping, which results from wave leakage, is not significantly affected by the dissipation of the numerical method.

5. Results

For simplicity, we have concentrated on perturbations located not too far from the loop (r_0 of the order of R). This is convenient because the initial disturbance is not significantly dispersed when it interacts with the tube. A highly dispersed wavetrain would lead to loop motions dominated by the wave passing through the loop (see Terradas, Oliver, and Ballester, 2005b). In addition, the loop will be able to confine more energy for perturbations situated close to the tube. This will facilitate the identification of the trapped eigenmodes in the time-dependent problem.

5.1. Sausage Modes

Sausage modes are leaky in the limit of a thin tube. For this reason, it is interesting to start with these modes since there are no trapped modes that can dominate the long-term behaviour. We have imposed that $m = 0$ and we have investigated the effect of an initial perturbation on the tube. We have first started with a purely Gaussian perturbation ($k_r = 0$).

In Figure 1 the radial velocity at the initial stages of the time evolution is represented. The initial perturbation (Figure 1a) splits into two pulses, one travelling towards and another travelling away from the loop. The amplitude of the pulse decreases for the disturbance propagating away from the loop and increases for the wave propagating towards the loop (see the height of the two peaks in Figure 1b). This is purely an effect of the cylindrical geometry. The pulse reaches the loop (located at $0 < r < R$) and transmission and reflection of the disturbance occur. The reflected part of the perturbation changes sign (see the peak around $r/R \approx 3$ in Figure 1c) and propagates away from the loop. The transmitted pulse inside the tube undergoes several reflections and transmissions at the loop boundary. Each time that it reaches the loop boundary it loses part of its energy in the external medium. Consequently, because of this continuous leakage of energy the amplitude of the oscillations decreases with time. This can be appreciated in Figure 2, where the evolution of the system at later times is represented (see, for example, Figures 2c and 2d). Note also that the amplitude of the oscillations at a fixed time decreases towards the loop. This is simply because oscillations located far from the loop were emitted at earlier stages and consequently carried more energy and

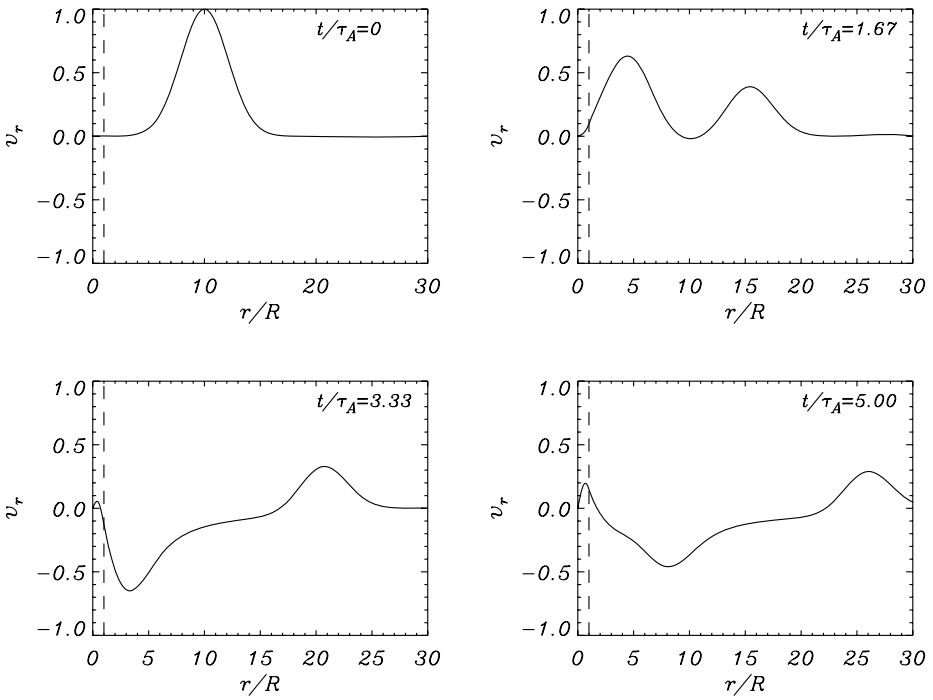


Figure 1 Radial velocity as a function of position for different times. The dashed line represents the loop boundary, located at $r/R = 1$. The loop length is $L = 100 R$ and the density contrast is $\rho_i/\rho_e = 10$. The initial perturbation is given by Equation (10) with $r_0 = 10 R$, $w = 3 R$, and $k_r = 0$. The distances are normalised to the loop radius R , and the time is normalised to the Alfvén crossing time $\tau_A = R/v_{Ai}$.

had a larger amplitude. This behaviour is in complete agreement with the spatial profile of the eigenfunction of the leaky modes (*i.e.*, increasing amplitude with r).

In Figure 3a the velocity profile at the loop boundary ($r = R$) is shown as a function of time. The signal shows a periodic behaviour and a strong attenuation of the amplitude of oscillation with time. The damping is produced by the continuous energy radiation in the external medium described before. The period and the damping time calculated from the simulations are in quite good agreement with those predicted for the trig leaky modes. We find that the period is $2.87\tau_A$ whereas the damping time (calculated from an exponential fit; see the dashed-dotted line in Figure 3a) is $4.17\tau_A$. The numerical solution of the dispersion relation gives values of $2.76\tau_A$ and $4.23\tau_A$, whereas the values of the approximate expressions [Equations (6) and (7)] are $2.67\tau_A$ and $3.16\tau_A$ for the period and damping times, respectively. In Figure 3b the wavelet transform (Torrence and Compo, 1998) of the signal is displayed. We see that the frequency smoothly increases until it reaches a value around the frequency of the first leaky mode. As expected, the power of the peak decreases with time owing to the attenuation of the amplitude of oscillation (for $t/\tau_A \geq 5$).

The results of a different initial excitation (with $k_r R = 1.25$) are plotted in Figure 4. The signal (see Figure 4a) is more complicated because of the superposition of the two different frequencies (see the wavelet transform in Figure 4b). Now instead of a single dominant leaky mode two radiating trig modes (the fundamental and the first harmonic) are excited at the same time. It is possible to see that both modes have approximately the same damping time. The power of the first harmonic is larger than that of the fundamental mode. Thus, the

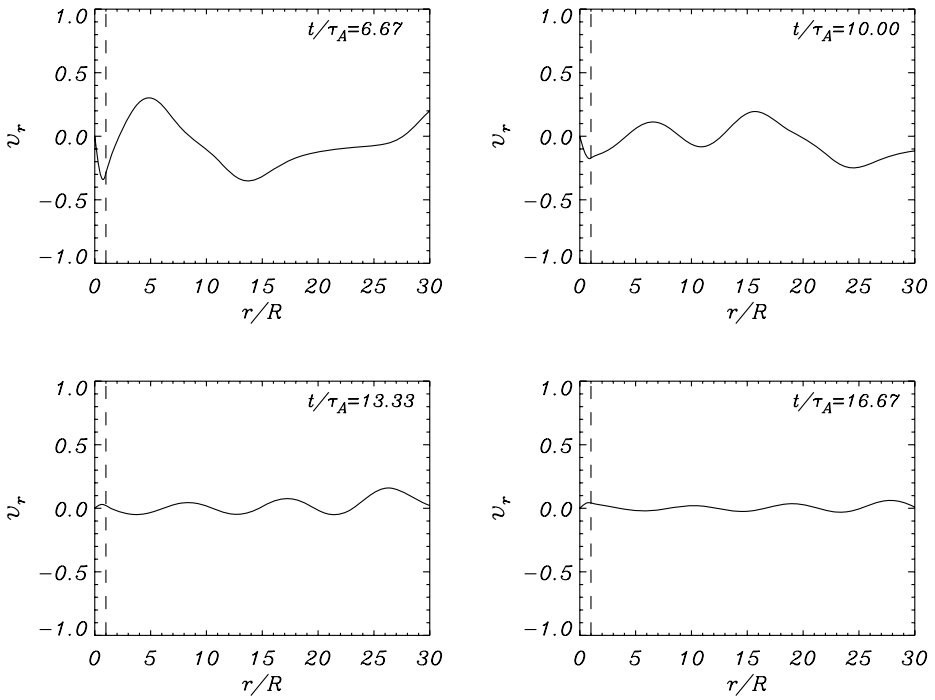


Figure 2 Radial velocity as a function of position for different times for the same simulation as in Figure 1 at later stages. Note that the amplitude of the oscillations decreases with time.

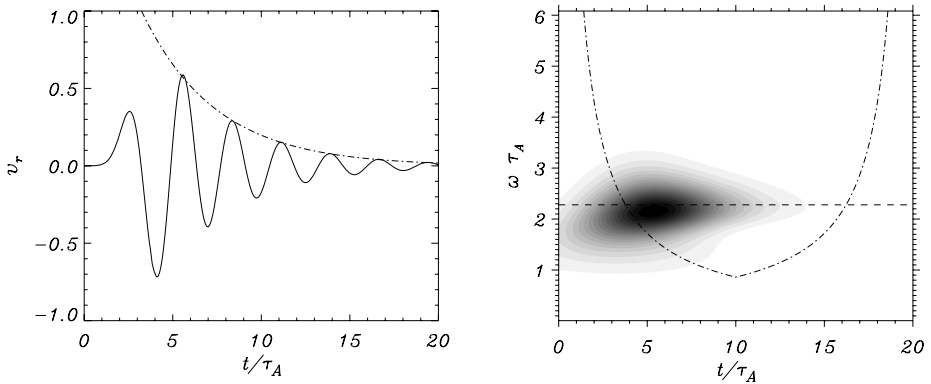


Figure 3 Left panel: Radial velocity as a function of time at $r = R$ for the simulation shown in Figure 1. The dash-dotted line is an exponential fit of the form e^{-t/τ_d} . Right panel: Wavelet transform of the signal. The dashed line corresponds to the frequency of the first leaky mode calculated from the dispersion relation. The dash-dotted line represents the cone of influence (COI).

excitation of the different leaky modes depends on the dominant wavelengths of the initial waveform. For this reason, it is interesting to study the power of the dominant peak in the wavelet transform as a function of the wavenumber k_r . This basically represents the response function of the loop for different initial perturbations with a dominant wavelength $2\pi/k_r$.

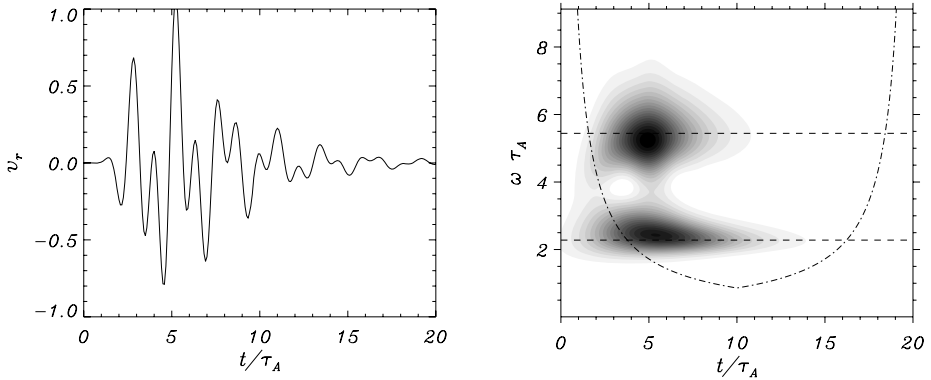
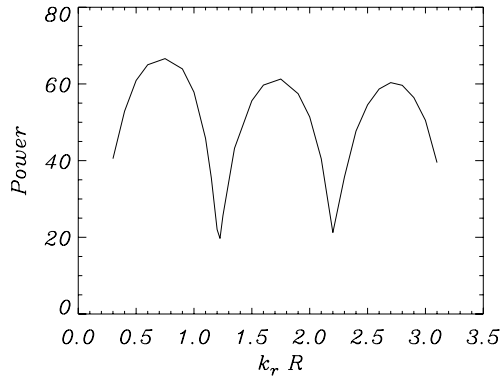


Figure 4 Left panel: Radial velocity as a function of time at $r = R$ with the same parameters as in Figure 1 but now with $k_r R = 1.25$. Right panel: Wavelet transform of the signal. The dashed lines correspond to the frequencies of the first two leaky modes calculated from the dispersion relation.

Figure 5 Power of the dominant peak in the wavelet transform (of v_r at $r = R$) as a function of $k_r R$. The maxima are associated with the leaky modes calculated from the normal mode analysis. In this plot $r_0 = 20 R$, $w = 6 R$.



The results are plotted in Figure 5 and we can see that the power shows several maxima. The peaks in the power are precisely located at the wavelengths that correspond to the leaky modes. This is very closely related to the bumps in the spectral measure in the treatment of Andries and Goossens (2007). In fact, if Figure 5 would be reconstructed using a very broad wavepacket in the initial condition (close to a δ distribution in k space) it would accurately represent the theoretical measure.

5.2. Kink Modes

In contrast the sausage modes, the kink modes ($m = 1$) are trapped even in the thin-tube approximation. Therefore, we expect that part of the energy of the initial perturbation will be trapped while another part will be radiated through the excitation of the leaky modes. An additional interesting feature is the possible excitation of the PFLK.

The results of the initial excitation are plotted in Figure 6. Now the signal initially shows a short transient phase ($0 \leq t/\tau_A \leq 20$), which is followed by a long-period oscillation. This oscillation is due to the excitation of the trapped kink mode. Its frequency is simply the kink frequency of the tube (see the dashed line in Figure 6b). The amplitude of the oscillation of the trapped mode remains constant with time. However, the initial transitory phase is

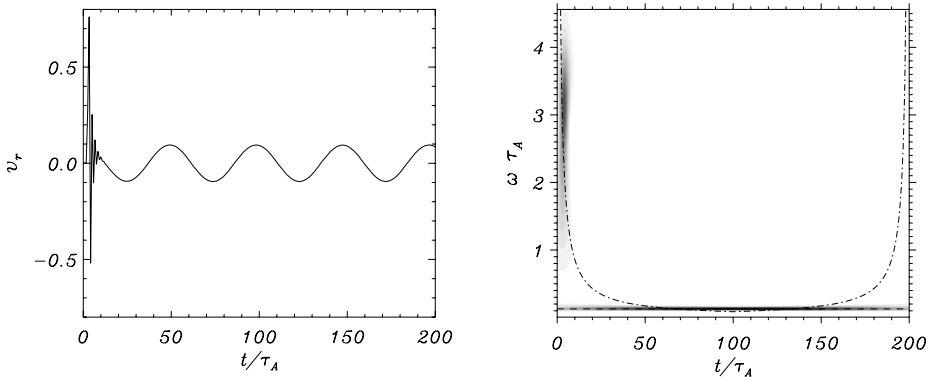


Figure 6 Left panel: Radial velocity as a function of time at $r = 0$. Right panel: Wavelet transform of the signal. After a short transient phase, the loop oscillates with the frequency of the kink mode. The loop length is $L = 30R$ and the density contrast is $\rho_i/\rho_e = 3$. The initial perturbation is given by Equation (10) with $r_0 = 5R$, $w = R$, and $k_r = 0$. The dashed line represents the frequency of the kink trapped mode calculated from the dispersion relation.

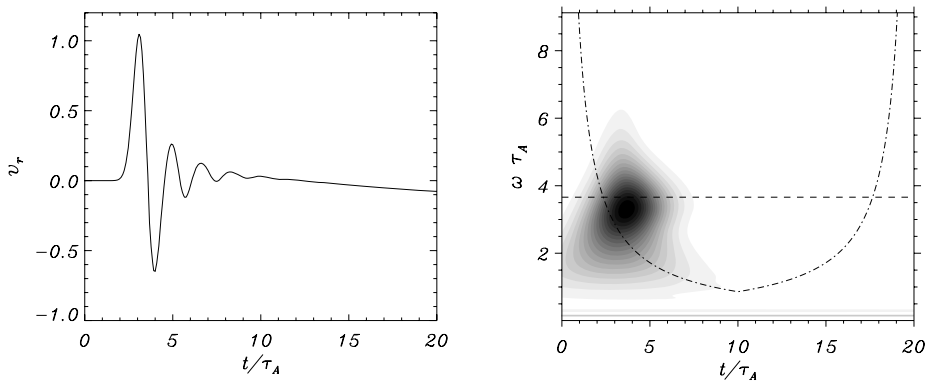


Figure 7 Left panel: Detail of the radial velocity plotted in Figure 6 in the range $0 \leq t/\tau_A \leq 20$. Right panel: Wavelet transform of the signal. The leaky mode is clearly identified and there is some indication of the trapped mode in the power spectrum.

associated with the leaky modes. In Figure 7 it is represented in more detail. Like for the sausage modes, the period of the transient phase is in agreement with the period of the (fundamental) kink leaky trig mode. Note that the amplitude of oscillation of the leaky transient is much larger than that of the trapped solution. These results are completely equivalent to those found in the slab model studied by Terradas, Oliver, and Ballester (2005a).

We have performed a similar simulation but now with an initial perturbation that is narrower (and consequently wider in k space). The results at the initial stages are represented in Figure 8. For the sausage modes, for this particular initial excitation, more than one single leaky mode is excited. Thus, the shape of the initial perturbation determines which leaky modes will be excited. The present perturbation is quite narrow in space, so its Fourier transform is wide in k , which explains why several trig leaky modes are excited. In addition, it is possible to see that for this perturbation less energy is deposited in the trapped eigenmode.

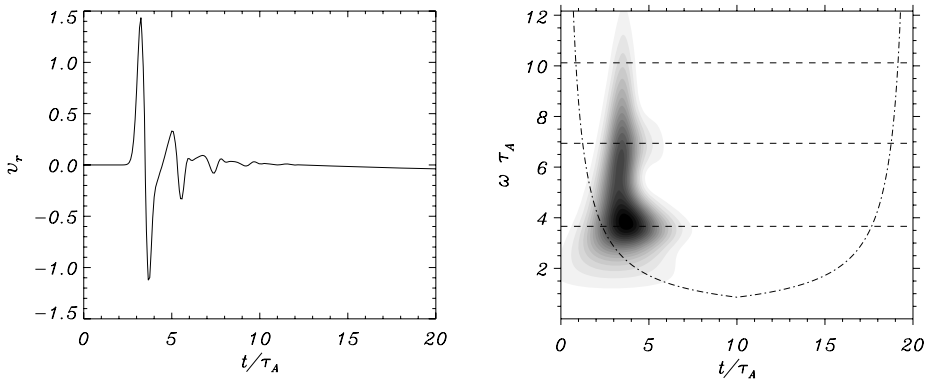


Figure 8 Left panel: Radial velocity as a function of time at $r = 0$ for a simulation in the same model as in Figure 6 but with $w = 0.5 R$. Right panel: Wavelet transform of the signal. The dashed lines correspond to the frequencies of the first three trig leaky kink modes calculated from the dispersion relation.

How the amount of energy of the trapped modes depends on the initial condition has been analysed by Terradas, Andries, and Goossens (2007), who also use a cylindrical-tube model.

Although the excitation of the trig modes is clear from the time-dependent problem, we have not found the orphan mode and the Type II trig modes. This is possibly due to their extremely fast damping time in comparison with their period. For example, the orphan mode has a period of $5.14\tau_A$ and a damping time of $0.61\tau_A$ (for a density contrast $\rho_i/\rho_e = 3$), whereas for the fundamental Type II mode the values are $-1.77\tau_A$ and $0.45\tau_A$.

Finally, we have investigated the possible excitation of the principal leaky mode. In the thin-tube limit the period of the trapped modes and PFLK are quite similar and the damping time of the principal leaky mode is quite long (small attenuation). This can make the identification of the radiating mode very difficult from the numerical simulations. For this reason, we have selected conditions for which the damping time is not long in comparison with the period (short and fat loops). In fact, for this situation the radial phase velocity of the principal leaky mode is not as small as in the thin-tube approximation, which in principle could help to excite these modes. Nevertheless, even under these conditions, we have not been able to find the PFLK. In Figure 9 the results are displayed for a particular case. We see that after a transient behaviour the loop eventually oscillates with the trapped mode. The period and the damping time of the principal leaky mode calculated from the dispersion relation are $15.61\tau_A$ and $62.89\tau_A$, respectively [$14.14\tau_A$ and $58.07\tau_A$ according to Equations (8) and (9)]. If there were attenuation at the frequency of the kink mode owing to the leaky mode it should in principle be detectable in Figure 9a. We see that the amplitude of oscillation is constant with time and therefore there are, apparently, no signatures of the principal leaky mode. However, the question that arises is whether the amplitude of this mode is large enough to be detected. In any case, it is clear that the behaviour of the loop is dominated by the trapped solution.

6. Conclusions

By solving the time-dependent problem, we have studied the problem of the excitation of coronal loop oscillations. We have found that the response of the loop to an external perturbation is characterised by short-period oscillations associated with leaky waves. The period

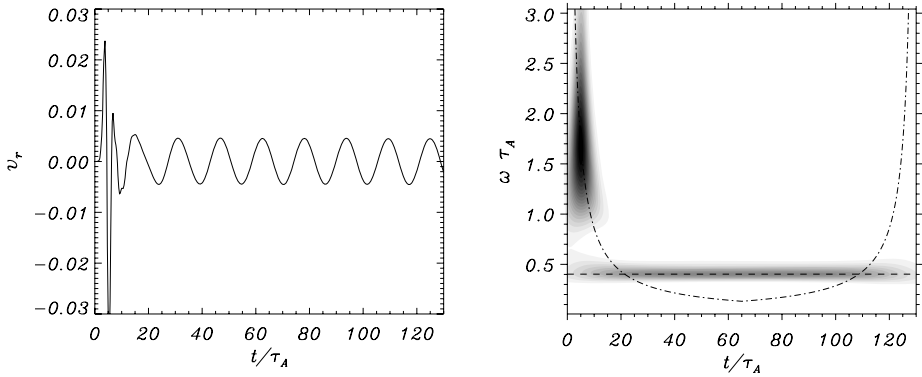


Figure 9 Left panel: Radial velocity as a function of time at $r = 0$. Right panel: Wavelet transform of the signal. After a short transient phase, the loop oscillates with the frequency of the kink mode. There is no signature of the excitation of the PFLK. The loop length is $L = 10 R$ (short loop) and the density contrast is $\rho_i/\rho_e = 6$. The initial perturbation is given by Equation (10) with $r_0 = 10 R$, $w = 3 R$, and $k_r = 0$. The dashed line represents the frequency of the kink trapped mode calculated from the dispersion relation.

and the damping time of these oscillations are in perfect agreement with the normal-mode calculations of the trig leaky or radiating modes. After this impulsive leaky phase, the loop oscillates with the corresponding trapped eigenmode, which has a much longer period than the leaky transient phase, and an amplitude that is constant with time.

Not all the solutions of the dispersion diagram are detected when the IVP is considered. In particular, we have not found any clear indication of the excitation of the principal leaky mode. We have shown that the system is always oscillating with a trapped solution (if this solution is allowed in the dispersion diagram) and that from all the possible leaky modes, at least the trig modes are physically relevant, since they are part of the time-dependent solution.

If leaky modes can be identified, then they can be also used as a tool to perform coronal seismology. This has been also suggested in another context by Verwichte, Foullon, and Nakariakov (2006). On one hand, we have shown that these modes have very large amplitudes in comparison with the amplitude of the trapped solution, but on the other hand, they have really short periods and attenuate very rapidly which makes them difficult to detect. However, with the recent radio-band observations with time resolution of the order of seconds these modes could in principle be detected.

Finally, it is important to note that we have concentrated on perturbations generated close to the loop. If the initial pulse is very dispersed, for example for perturbations generated far from the tube (or for perturbations located close to the tube but for short loops, *i.e.* k_z large), the behaviour can be quite different. This issue was investigated by Terradas, Oliver, and Ballester (2005b) in a slab model and it was shown that the loop moves with the wavetrain of the disturbance. As a consequence, the loop basically oscillates with the external cutoff frequency and its motion is attenuated due to the wake of the travelling disturbance. A negligible amount of energy is deposited in the trapped mode. This problem needs to be explored further in the cylindrical geometry.

Acknowledgements J. Terradas is grateful to the K.U. Leuven (Department of Mathematics) for a post-doctoral fellowship. He also thanks the Spanish Ministry of Education and Science for the funding provided under a Juan de la Cierva fellowship and for funding provided under Grant No. AYA2006-07637.

References

- Andries, J., Goossens, M.: 2007, *Phys. Plasmas* **14**, 052101.
- Aschwanden, M.J., Fletcher, L., Schrijver, C.J., Alexander, D.: 1999, *Astrophys. J.* **520**, 880.
- Aschwanden, M.J., De Pontieu, B., Schrijver, C.J., Title, A.M.: 2002, *Solar Phys.* **206**, 99.
- Cally, P.S.: 1986, *Solar Phys.* **103**, 277.
- Cally, P.S.: 2003, *Solar Phys.* **217**, 95.
- Cally, P.S.: 2006, *Solar Phys.* **233**, 79.
- Edwin, P.M., Roberts, B.: 1983, *Solar Phys.* **88**, 179.
- Pascoe, D.J., Nakariakov, V.M., Arber, T.D.: 2007, *Astron. Astrophys.* **461**, 1149.
- Roberts, B., Edwin, P.M., Benz, A.O.: 1984, *Astrophys. J.* **279**, 857.
- Ruderman, M.S., Roberts, B.: 2006a, *J. Plasma Phys.* **72**, 285.
- Ruderman, M.S., Roberts, B.: 2006b, *Solar Phys.* **237**, 119.
- Schrijver, C.J., Aschwanden, M.J., Title, A.M.: 2002, *Solar Phys.* **206**, 69.
- Sewell, G.: 2005, *The Numerical Solution of Ordinary and Partial Differential Equations*, Wiley-Interscience, New York.
- Spruit, H.C.: 1982, *Solar Phys.* **75**, 3.
- Stenuit, H., Keppens, R., Goossens, M.: 1998, *Astron. Astrophys.* **331**, 392.
- Stenuit, H., Tirry, W.J., Keppens, R., Goossens, M.: 1999, *Astron. Astrophys.* **342**, 863.
- Terradas, J., Andries, J., Goossens, M.: 2007, *Astron. Astrophys.* **469**, 1135.
- Terradas, J., Oliver, R., Ballester, J.L.: 2005a, *Astron. Astrophys.* **441**, 371.
- Terradas, J., Oliver, R., Ballester, J.L.: 2005b, *Astrophys. J.* **618**, L149.
- Torrence, C., Compo, G.P.: 1998, *Bull. Am. Meteorol. Soc.* **79**, 61.
- Verwichte, E., Foullon, C., Nakariakov, V.M.: 2006, *Astron. Astrophys.* **452**, 615.
- Wilson, P.R.: 1981, *Astrophys. J.* **251**, 756.